Hydrogeology Journal (2023) 31:1847–1861
https://doi.org/10.1007/s10040-023-02663-0

REPORT

Multi-technique approach for estimating groundwater transit time through the saturated zone of an unconfined granular aquifer in Quebec, Canada

Chaima Miled[1,2] · Romain Chesnaux[1,2] · Julien Walter[1,2] · Lamine Boumaiza[3] · Maxime C. Paré[4]

Received: 18 October 2022 / Accepted: 18 June 2023 / Published online: 5 August 2023

Abstract
Agricultural activities can generate contaminants that enter underlying granular aquifers and become transported within the groundwater to adjacent streams. This paper reports on estimation of the transit time of groundwater through a saturated granular unconfined aquifer in an agricultural region of Saguenay-Lac-Saint-Jean, Quebec (Canada). A multi-technique approach is applied, integrating analytical, hydrogeochemical, and numerical methods—to determine groundwater flow from a recharge (wetland) to discharge zone (groundwater seep). Fieldwork observations, including borehole drilling, soil/groundwater sampling, and piezometers, were combined with laboratory measurements of soil hydrogeological properties and stable ($\delta^{18}O_{H2O}$ and $\delta^{2}H_{H2O}$)/radioactive (^{3}H) isotopes in the collected groundwater. The Dupuit–Forchheimer-based analytical method used here estimated a groundwater transit time of 7.75 years, whereas the hydrogeochemical-based and three-dimensional FEFLOW numerical method produced estimates of 7.34 and 7.27 years, respectively. The similarity of the three estimates highlights the robustness of the approach, which integrates field data to produce accurate assessments of groundwater transit time. This multi-technique approach will help in the sustainable management of groundwater resources and for preparing effective environmental plans for agricultural practices in areas underlain by aquifers.

Keywords Analytical solution · Groundwater recharge · Hydrogeochemistry · Canada · Tritium

Introduction

Groundwater plays an integral role in the water cycle by connecting surface-water ecosystems, contributing to river and stream flows, and irrigating food resources used by terrestrial fauna (Boumaiza et al. 2020c; Ritter et al. 2002; Zedler and Kercher 2005). When contaminants are released into the subsurface, mechanisms such as advection, dispersion, and diffusion transport the introduced substance within the aquifer over distances of several meters to tens of kilometers (Bradley 2013; Gorelick et al. 1993). The amount of contaminant transported into the subsurface depends on the nature of the contaminant, the aquifer geology, and groundwater flow (Boumaiza et al. 2022a; McCarthy and Zachara 1989). The transit time of the contaminant can be defined in two ways. First, transit time through the aquifer vadose zone represents the time required for the contaminant to reach the water table from the ground surface (Sousa et al. 2013). The second concept refers to the transit time of a parcel of water from its recharge at the water table to its discharge along a stream bed or spring (Cartwright and Morgenstern 2016). Knowing the transit time of a contaminant permits evaluating the potential movement of groundwater contamination.

Over the past few decades, considerable research has been devoted to investigating groundwater transit times (Boumaiza et al. 2021a; McGuire and McDonnell 2006). Isotopic signatures have been used effectively to trace groundwater transit in aquifers. For example, Małoszewski et al. (1983) and Vitvar and Balderer (1997) used water

✉ Chaima Miled
chaima.miled1@uqac.ca

1 Département des Sciences Appliquées, Université du Québec à Chicoutimi, Saguenay, Québec G7H 2B1, Canada

2 Centre d'études sur les ressources minérales, Groupe de recherche Risque Ressource Eau, Saguenay, Québec G7H 2B1, Canada

3 Department of Earth and Environmental Sciences, University of Waterloo, Waterloo, ON N2T 0A4, Canada

4 Département des Sciences Fondamentales, Laboratoire sur les écosystèmes terrestres boréaux (EcoTer), Université du Québec à Chicoutimi, Saguenay, Québec G7H 2B1, Canada

isotopic content ($\delta^{18}O_{H2O}$ and $\delta^{2}H_{H2O}$) and data on solutes in precipitation and stream water to estimate transit time. These studies were limited however by (1) the poor quality of the data series, (2) the short length of the observational record, and (3) the sample collection strategy. The application of natural tracers to determine groundwater circulation is widely documented (Clark and Fritz 1997; Cook and Herczeg 2012; Mazor 2003). Some environmental tracers such as carbon-14 (^{14}C) and tritium (^{3}H) are used to estimate groundwater transit time, whereas other tracers can reveal the origin of flows, groundwater mixing, and mineralization (Fontes 1992). Tritium (^{3}H) has been used to determine the transit times of shallow groundwater, soil water, and surface water (Cartwright and Morgenstern 2015, 2016; Cook and Böhlke 2000). When ^{3}H activity is combined with models that describe the distribution of flow paths within an aquifer (Cook and Böhlke 2000), transit time estimates, up to ~100 years old, can be provided for groundwater.

Multi-tracer approaches have been widely used over the last two decades (Ekwurzel et al. 1994; Gillon et al. 2012; Lefebvre et al. 2015; Mazariegos et al. 2017). Applying several tracers allows for the identification of groundwater processes (e.g., mixing processes, dispersion, degradation, contamination) that could have been misinterpreted or not observed through use of a single tracer.

Furthermore, the continual development of analytic expressions has made it possible to describe horizontal and vertical flow velocities, age profiles, and fluxes such as recharge (Chesnaux 2013; Chesnaux et al. 2021; Cook and Böhlke 2000; Vogel 1967). One of the earliest models was that of Vogel (1967) which provided a solution based on Darcy's law for the vertical distribution of hydraulic age in an unconfined aquifer characterized by uniform recharge and constant thickness. Cook and Böhlke (2000) summarized the range of analytical solutions available for determining hydraulic age; however, these analytical solutions are only required for homogeneous flow systems. Analytical models can also now combine a hydraulic simulation with an advection–dispersion solution to describe tracer movements within groundwater flow (Bethke and Johnson 2008; Leray et al. 2012).

Multiple numerical methods are available for estimating groundwater travel times (Cornaton 2003; Goode 1996). Goode (1996) applied a numerical advective–dispersive transport model to derive an equation for determining groundwater age and groundwater mass. Cornaton (2003) and Etcheverry and Perrochet (2000) applied residence time theory to produce deterministic models of groundwater age. Despite being widely applicable, numerical techniques for solving groundwater transit time require more computational resources; however, they are appropriate for modeling more complex aquifer systems.

Many studies have focused on estimating groundwater transit time using a single approach, whereas few have tried to combine different approaches (Basu et al. (2012). Although necessary for effective and sustainable groundwater management, studies combining different approaches are challenging because the multiple sources of input data require diverse measurements from relatively large aquifers. Hence, the collection of required field data is one of the most expensive, albeit valuable, tasks for estimating groundwater transit time.

This field-based study applies a multi-technique approach to estimate groundwater transit time through an unconfined granular aquifer. The approach integrates (1) an analytical-based solution, developed by Chesnaux et al. (2005) to calculate groundwater travel times in the configuration of a Dupuit–Forchheimer type flow system (Bear 1972b, 1988; Dupuit 1863; Forchheimer 1886) in an unconfined aquifer, (2) a hydrogeochemical technique involving environmental tracers ($\delta^{18}O_{H2O}$, $\delta^{2}H_{H2O}$, and ^{3}H), and (3) numerical modeling for which field observations are used to calibrate the developed model. The aquifer lying within an agricultural experimental site, Bleuetière d'Enseignement et de Recherche (BER) in Quebec (Canada), was selected because agricultural practices can generate contaminants that are transported through the granular aquifer to reach the surrounding rivers. Note that there are no pumping activities, irrigation, or other possible human activities that may influence recharge on this site. Collected field data from BER combined with diverse techniques heightens the accuracy of transit time estimates. This improved estimate is valuable for groundwater researchers/managers for preparing effective environmental plans for agricultural regions. This study aims to characterize the BER site's aquifer, undergoing commercial wild blueberry activity, by (1) estimating groundwater recharge and (2) evaluating the transit time of groundwater through the aquifer system.

Materials and methods

Study area

Bleuetière d'Enseignement et de Recherche is an experimental scientific research site managed by the Université du Québec à Chicoutimi (Fig. 1). The site is located 10 km southwest of the town of Normandin in the Saguenay-Lac-Saint-Jean region (SLSJ) of Quebec, Canada. The 55-ha study site is an agricultural field covered by crops of wild blueberries (*Vaccinium angustifolium* Aiton and *V. myrtilloides* Michx). Regional climate is characterized by hot, humid summers, cold, snowy winters, and wet springs and autumns. Mean annual precipitation is approximately 967 mm. Average temperatures range from –15.2 °C in winter to 18.9 °C in summer (Government of Quebec 2022).

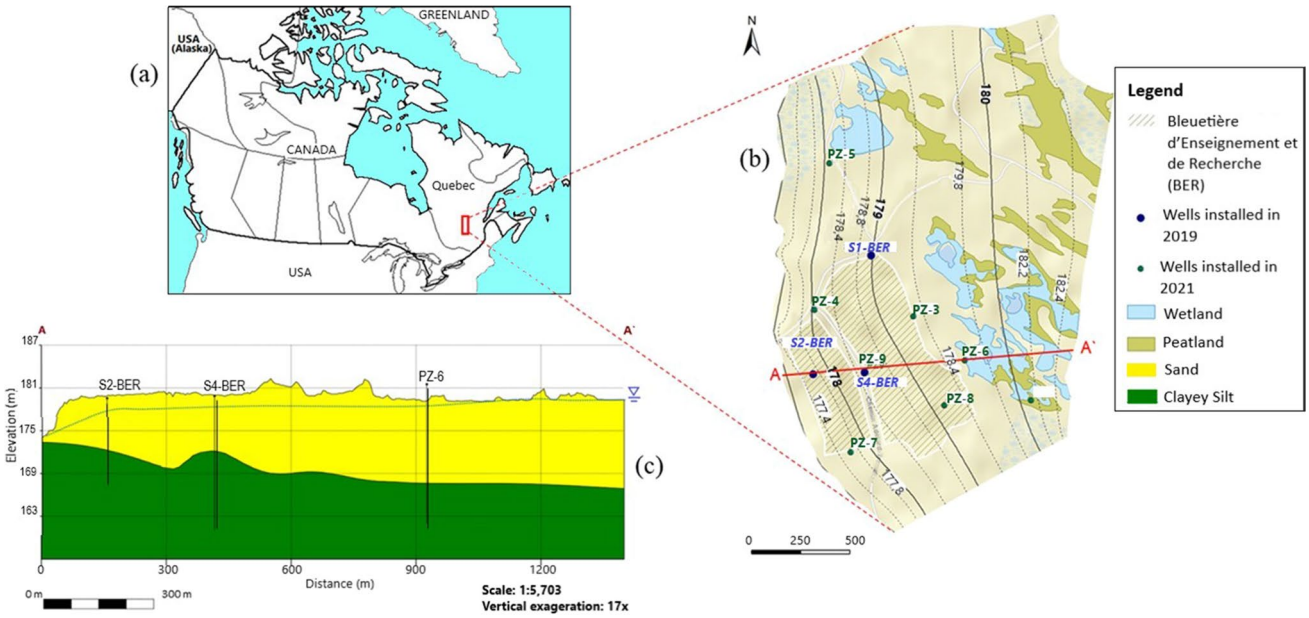

Fig. 1 **a** Location of the study site in Québec (Canada); **b** locations of the installed observation wells, showing the location of the cross-section, the surface cover, and equipotential lines at the Bleuetière d'Enseignement et de Recherche (BER) site; **c** stratigraphic cross-section A–A′ with subsurface materials and the location of studied wells

Bleuetière d'Enseignement et de Recherche lies on unconsolidated Quaternary deposits that overlie the crystalline bedrock of the Grenville Province. The Quaternary sediments date to the last glacial and deglacial period. Following the retreat of the Laurentide Ice Sheet about 11,800 years ago, the Laflamme Sea inundated much of the SLSJ region (LaSalle and Tremblay 1978), leaving deep-water marine deposits consisting of grey clay or clayey silt. The BER aquifer, maximum thickness of 14 m, comprises proglacial deltaic sands and silt deposited over an aquitard composed of clayey silt from the Laflamme Sea (Fig. 1). The surface of the unconfined aquifer is characterized by relatively flat topography, wetlands in the eastern portion of the BER, and a thin vadose zone of variable thickness, 0.5–2.5 m below ground surface (bgs).

Field sampling and laboratory analyses

Soil sampling

Three boreholes were drilled at the study site in October 2019 to serve as the observation wells S1-BER, S2-BER, and S4-BER with depths of 8.23, 6.71, and 12.19 m bgs, respectively (Courchesne 2019). In July 2021, four additional boreholes (PZ-1, PZ2, PZ3, and PZ4) were drilled to a maximum depth of 5 m using a hand threshing beating auger and were then equipped with observation well installations (Fig. 1).

During borehole drilling, continuous soil samples were collected from the split-spoon sampler (0.69-m long, 0.05-m diameter). These soil samples were collected at an average interval of 20 cm to obtain a high-resolution vertical profile. At each sampling, the split spoon was cleaned using dry towels to minimize intersample contamination. Following a visual description (sediment texture, colour, humidity) of the samples in the field, the collected samples were quickly stored in separately labelled polyethylene Ziploc bags, and tightly sealed to avoid moisture loss through evaporation.

Soil physical properties by drying

In the laboratory, all fresh soil samples were placed into individual metal cylinders of known weight and volume. Following their weighing, the soil samples were dried in an oven for 48 h at 105 °C. The dried-sample weight was then used to determine the total wet and dry soil mass. Gravimetric water content (GWC, expressed in %) was calculated for each soil sample (Gardner 1965). Dry bulk density (D_b), expressed in g cm^{-3}, was determined according to Black (1965) and the volumetric water content (VWC, expressed in %) was calculated following (Gardner 1965) and assuming a water density (ρ_w) of 1 g cm^{-3}. Soil porosity (n, expressed in %) was calculated using Black (1965) and assuming a particle density (ρ_p) of 2.69 g cm^{-3} for sand (Boumaiza et al. 2015, 2017, 2020b). The void ratio (e) was also determined. Parameters n and e were used to estimate the saturated hydraulic conductivity (K_s).

Soil physical properties by grain size

Successive soil samples of similar texture and structure were combined into a single sample. These grouped samples were analysed with grain-size sieves, and grain-size fractions were reported following the Wentworth classification (Wentworth 1922) and plotted as granulometric curves. The latter were used to estimate K_s using five empirical equations—i.e., Hazen (1983); Beyer (1964); Chapuis (2004); Sauerbrey (1932); U.S. Bureau of Reclamation (Milan and Andjelko 1992); Navfac (1974). These equations and their application limits are detailed in Table 1. Some empirical equations adopted in this study may not apply to certain soil samples because of different conditions of applicability related to void ratio and granulometry. Accordingly, K_s for each soil sample was calculated using only the applicable empirical equations and adopted a geometric mean value (Boumaiza et al. 2020a; Zappa et al. 2006). An equivalent saturated hydraulic conductivity (K_{eq}) value was determined for the full soil profile of each drilled borehole.

Groundwater sampling and isotope analyses

The groundwater sampling program included groundwater samples collected from four observation wells—PZ-6, S1-BER, S2-BER, and S4-BER—for isotope analyses (Fig. 1). Prior to sampling, stagnant groundwater present in the observation wells was purged using a pumping system. The physicochemical parameters—temperature (T), pH, and electrical conductivity (EC)—of the pumped groundwater were then monitored with a portable multi-parameter probe until three consecutive readings stabilized within ±10%. Once stable results were attained, groundwater samples were then collected. Groundwater destined for δ^2H_{H2O} and $\delta^{18}O_{H2O}$ analyses was collected in two 30-ml high-density polyethylene (HDPE) bottles, and water for ^3H activity was collected in 2,000-ml HDPE bottles. All samples were collected in bottles without headspace and fitted with Teflon septa parafilm-caps to prevent evaporation. The groundwater samples were stored in a cooler at 4 °C during fieldwork before being stored in a refrigerator. All groundwater samples were transported to the Environmental Isotope Laboratory (EIL) at the University of Waterloo, Ontario, Canada.

The δ^2H_{H2O} and $\delta^{18}O_{H2O}$ ratios were determined using a Los Gatos Research Triple Liquid Water Isotope Analyzer LGR T-LWIA 45-EP following the analytical scheme recommended by the International Atomic Energy Agency (IAEA; Penna et al. 2010). Groundwater samples for ^3H were degassed and stored in dedicated glass bulbs for the accumulation of the tritium decay product. For high-precision analyses, samples were enriched (ultra-low levels) 45–50 × by electrolyzing multiple additions of the sample followed by counting. The detection limit of ultra-low-level enriched samples is 0.1±0.1 TU (1 TU equals a radioactivity concentration of 0.118 Bq L^{-1}) at 2 sigma (at low levels) (Taylor 1976). The obtained ^3H activities were corrected for radioactive decay back to the time of the precipitation event, and ^3H activities are expressed in tritium units. The isotope ratios, expressed in permil (‰) using delta (δ) notation, were calculated using Eq. (1), where R_{sample} and $R_{standard}$ are the sample's and the standard's ratios, respectively, of the heavier to lighter isotope, i.e., $^2H/^1H$, $^{15}N/^{14}N$, or $^{18}O/^{16}O$.

Table 1 Selected empirical equations used to estimate K_s and the conditions necessary for their application

Method	Empirical formula for K_s (cm s^{-1})	Applicability conditions
Hazen	$(d_{10})^2$ with d_{10} in mm	Sand and gravel $C_u \leq 5$ 0.1 mm $\leq d_{10} \leq$ 3 mm
Chapuis	$2.4622((d_{10})^2e^3)/(1+e))^{0.7825}$ with d_{10} in mm	All natural soils without plasticity 0.003 mm $\leq d_{10} \leq$ 3 mm $0.3 \leq e \leq 1$
Sauerbrey	$2.436n^3 (d_{17})^2/(1-n)^2$ with d_{17} in mm	Sand and silty sand $d_{10} \leq$ 0.5 mm
Beyer	$0.45(d_{10})^2\log(500/C_u)$ with d_{10} in mm	Sand 0.06 mm $\leq d_{10} \leq$ 0.6 mm $1 \leq C_u \leq 20$
USBR	$0.36(d_{20})^{2.3}$ with d_{20} in mm	Sand and gravel $2C_u \leq 5$
NAVFAC DM7	$(d_{10})^{1.291e-0.6435} (d_{10})^{0.5504e-02937}$ with d_{10} in mm	Sand and mixtures of sand and gravel $2 \leq C_u \leq 12$ $d_{10}/d_5 \leq 3$ mm

d_x: effective grain size of x (% by weight of soil); C_u: coefficient of uniformity for non-plastic soils ($C_u = d_{10}/d_{60}$); *n:* Porosity

$$\delta = \left(\frac{R_{\text{sample}} - R_{\text{standard}}}{R_{\text{sample}}} \right) \quad (1)$$

Both δ^2H_{H2O} and $\delta^{18}O_{H2O}$ were reported relative to the Vienna standard mean ocean water (VSMOW), and the precision of the analytical instrument was generally better than ±0.8‰ for δ^2H_{H2O} and ±0.2‰ for $\delta^{18}O_{H2O}$. The distribution of δ^2H_{H2O} and $\delta^{18}O_{H2O}$ of the collected groundwater samples was compared to the range of the local meteoric water line (LMWL) derived from the local precipitation stable isotope data collected during the PACES program (Programme d'acquisition de connaissances sur les eaux souterraines).

Estimating groundwater recharge

Groundwater recharge was estimated using the analytical approach developed by Bear (1972b), an approach successfully applied by Chesnaux (2013) and Labrecque et al. (2020). The Bear (1972b) approach is based on the Dupuit–Forchheimer model (Dupuit 1863; Forchheimer 1886), which simplifies groundwater flows to a single dimension by assuming (1) the aquifer overlies a fully horizontal impervious substratum; (2) the aquifer is bound by two fixed-head boundaries; (3) the vertical component of groundwater velocity is neglected; and (4) the aquifer is considered homogeneous and isotropic, and steady-state conditions are assumed for the flow. This analytical approach relies on the general Bear (1972b) solution to Dupuit–Forchheimer's systems for the saturated groundwater thickness above the datum represented by the top of the impervious substratum underlying the aquifer. The solution is expressed as Eq. (2):

$$h(x) = \sqrt{-\frac{W}{K}x^2 + \left(\frac{h_L^2 - h_0^2}{L} + \frac{WL}{K}\right)x + h_0^2} \quad (2)$$

where h is the phreatic surface elevation, x represents the distance from the upstream aquifer boundary, W is the groundwater recharge (mm year^{-1}), L is the length of the aquifer [L], h_0 and h_L are the fixed upstream ($x = 0$) and downstream ($x = L$) heads, respectively (it is assumed that $h_0 > h_L$), K is the hydraulic conductivity of the aquifer [LT^{-1}], and $h(x)$ is the hydraulic head [L] along the x-axis.

The squared saturated thickness of the aquifer where the piezometers were installed was plotted as a function of distance along the flow line (A–A′). The hydraulic head in the aquifer can be calculated by applying a quadratic regression on the plot using Eq. (2). Introducing the estimated K_{eq} value into Eq. (2) permits calculating groundwater recharge from the constant coefficient of the polynomial regression model (Chesnaux 2013; Labrecque et al. 2020).

Groundwater recharge analytical-solution-based estimates were validated using the water-table fluctuation (WTF) method (Lanini and Caballero 2021; Lanini et al. 2016). Piezometric fluctuations were monitored between March 2021 and March 2022 at three observation wells (S1-BER, S2-BER and S4-BER). These wells were equipped with pressure sensors to monitor local fluctuations of the water table at 15-min intervals. The ESPERE program includes several commonly used tools to run simultaneously for estimating groundwater recharge. In ESPERE, the WTF is based on the RISE method described by Healy and Cook (2002), assuming continuous aquifer drainage on an event basis as suggested by Nimmo et al. (2015). The annual groundwater recharge estimated by the WTF-based method equals the sum of all increases in water-table elevation and corrections during the year; it is estimated using Eq. (3).

$$R = S_y \sum (\Delta h + \delta) \quad (3)$$

where R is the groundwater recharge (mm year^{-1}), S_y represents the specific yield, δ is the interpolated exponential recession, and $\Delta \boldsymbol{h}$ is the head defined by the water level rise (D_H) over time (D_t).

Estimating groundwater transit time

Analytical approach

Travel time was assessed analytically using a closed-form analytical solution developed by Chesnaux et al. (2005). This analytical solution considers the configuration of an unconfined aquifer under Dupuit–Forchheimer conditions (Bear 1972a; Forchheimer 1886) assuming a steady-state regime, saturated flow through a horizontal aquifer experiencing a constant groundwater recharge, and groundwater discharge to a downgradient fixed-head boundary. Chesnaux et al. (2005) considered two cases: case I applies to flow systems containing a flow divide between two fixed-head boundaries, whereas case II refers to unidirectional flow between an upstream and downstream constant head boundary. Case II (Fig. 2) was adopted. A transformation was applied to the flow system by placing the upstream head, i.e., the upgradient water divide (Fig. 2), at the origin of the flow system. The application of case II is constrained between x = 0 and $x = L$; however, the solution transformed the flow system between $x = |xWD|$ and $x = L + |xWD|$, where $L + |xWD| = L'$, and L' represents the length of the transformed flow system. Accordingly, the travel time is only representative of the original flow system between $x = |xWD|$ and $x = L'$. Equation (3) represents the analytical solution developed by Chesnaux et al. (2005), where K is the hydraulic conductivity of the aquifer [LT^{-1}], W is the aquifer recharge [LT^{-1}], L' is the length of the aquifer [L], n_e is the effective porosity of the aquifer, and $h_{L'}$ is the constant head boundary discharge [L]. The prefix α in Eq. (5) is calculated using Eq. (4).

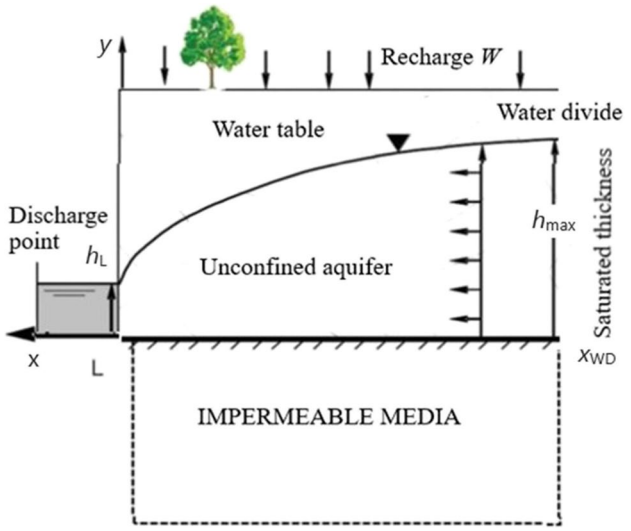

Fig. 2 Conceptual model of flow in a uniformly recharged, unconfined horizontal aquifer, where groundwater flow is unidirectional and unidimensional between the upstream and downstream constant head boundaries. Adapted from (Chesnaux 2013; Chesnaux et al. 2005)

$$t(x) = n_e \sqrt{\frac{\alpha}{K \cdot W}} \left[x\sqrt{\frac{1}{x^2} + \frac{1}{\alpha}} - x_i \sqrt{\frac{1}{x^2} + \frac{1}{\alpha}} + \ln\left(\frac{\sqrt{\frac{\alpha}{x_i}} + \sqrt{\frac{\alpha}{x_i^2} - 1}}{\sqrt{\frac{\alpha}{x}} + \sqrt{\frac{\alpha}{x^2} - 1}} \right) \right] \quad (4)$$

where

$$\alpha = L^2 + \frac{K \cdot h_{L'}^2}{W} \quad (5)$$

Hydrogeochemical approach

The radioactive decay method (Clark and Fritz 1997) was applied to date groundwater. Dating of groundwater by ^{3}H decay assumes a known tritium input into the groundwater and that the residual tritium, which is measured in the groundwater sample, is the result of decay. The decay is calculated using Eq. (6).

$$a_t{}^3\mathrm{H} = a_0{}^3\mathrm{H} \times e^{-\lambda t} \quad (6)$$

where $a_0{}^3$H is the initial tritium activity or concentration (expressed in TU), $a_t{}^3$H is the activity (measured in a groundwater sample) remaining after decay over time t, and λ represents the decay term calculated via Eq. (7), where the half-life $t_{1/2}$ equals 12.43 years.

$$\lambda = \frac{\ln 2}{t_{\frac{1}{2}}} \quad (7)$$

Finally, Eq. (6) can be rewritten as

$$t = -17.93 \times \frac{a_t{}^3\mathrm{H}}{a_0{}^3\mathrm{H}} \quad (8)$$

The value of $a_0{}^3$H was determined online from a member station of the Global Network of Isotopes in Precipitation (GNIP) database, operated by the International Atomic Energy Agency (Aggarwal et al. 2010). Here, ^{3}H monthly data are available from August 1953 to March 2019 from the closest GNIP-member station (Ottawa, ON), located approximately 453 km southwest of the study site. The initial tritium concentration ($a_0{}^3$H) data set was chosen to coincide with the recharge potential period suggested by the stable water isotope signatures obtained in this study and to validate the travel time result obtained from the analytical model.

Numerical approach

A numerical-based approach developed using FEFLOW-3D code (Version 7.5; Diersch 2013) was applied. A geological model was initially built using Leapfrog Geo (Seequent 2022) and then integrated within FEFLOW-3D to conduct numerical groundwater flow simulations (Diersch 2013). Numerous studies have confirmed the robustness of these codes (Hudon-Gagnon et al. 2011; Larocque et al. 2019; Nastev et al. 2005).

For these analyses, the entire 55 ha study area was modeled. Maximum depth for the model was 22 m as the natural impermeable substratum has been investigated to this depth. FEFLOW-3D modelling requires information on the horizontal/vertical distribution of hydrofacies to distinguish permeable/impermeable lithofacies within the modeled area. The modeling requires certain input parameters including hydraulic conductivity and porosity. The model is divided into two layers for which the attribution of the hydrogeological parameters is imported as shape files prepared previously in ArcGIS. Two layers were selected: (1) the aquifer, assumed as homogeneous, and (2) the impermeable substratum. The introduced values for hydraulic conductivity and porosity were those obtained from the sieve grain analyses. Once the modelled domain was established, the TetGen mesh generator, included in FEFLOW code, was run in order to generate a finite element mesh comprising tetrahedral elements. The steady-state condition was set for the established model, which was constrained by specific boundary conditions. A Dirichlet boundary condition was set by inputting head values on the eastern and western model boundaries. The eastern boundary of the aquifer consisted of a wetland area; this boundary is assumed to be acting as a groundwater divide. The western boundary represents the discharge area where groundwater seeps out of the point of contact between the aquifer and the aquitard, whereas the northern and southern limits of the study site were assigned without

any specification. Therefore, these limits were deemed as impermeable borders, as there were no obvious boundaries observed on the field site. The study site was modeled as a domain receiving a uniform spatial recharge, a parameter adopted from the results of the present study, i.e., the groundwater recharge value estimated analytically by the Dupuit–Forchheimer solution.

Model performance based on the available head observations was evaluated with several statistics that rely on the error of the model mass balance and the root mean squared error (RMSE). The RMSE measured the deviation between the simulated and observed water levels within the site's observation wells and is defined as

$$\mathrm{RMSE} = \sqrt{\frac{\sum_{i=1}^{m} (y_i - O_i)^2}{m}} \tag{9}$$

where m is the number of observations, and O_i and y_i are the observed and predicted data, respectively.

The forward particle-tracking option of the FEFLOW-3D code is a postprocessing tool that calculates the pathway and transit time for an introduced particle (Anderson et al. 2015). Particle tracking is generally used for representing the advective transport of solutes and contaminants (Anderson et al. 2015). Here, standard streamlines were applied because they represent trajectories of particles flowing by advective velocity within steady-state conditions; the particle tracking between two specified points corresponds to transit time.

Results

Aquifer stratigraphy from the collected soil samples

The sediment material at the drilled boreholes varied only slightly among sites and matching samples recovered in an earlier study (Courchesne 2019), demonstrating the relative homogeneity of the granular aquifer (Table 2). Samples were dominated by fine-to-medium coarse sands with traces of silt and gravel.

Calculated hydrogeological properties

Grain-size sieve analysis (Fig. 3) using the Wentworth (1922) classification revealed that the aquifer is generally composed of fine-to-medium coarse sands with traces of silt and gravel. Using obtained grain-size curves—see the electronic supplementary material (ESM)—and estimated soil properties (i.e., porosity and void ratio), the average K_s for each combined soil sample was determined. The K_s values were calculated using selected empirical equations (Table 1), and then the calculated K_s values were averaged to obtain a value $K_{s.eq}$ assumed to represent the entire aquifer. The obtained $K_{s.eq}$(4.65×10^{-4} m s^{-1}) was comparable to previous estimates for sites S1 (6.4×10^{-4} m s^{-1}) and S2 (4.5×10^{-4} m s^{-1}) situated in adjacent aquifers (Boumaiza 2008; Boumaiza et al. 2019, 2020b).

After applying the analytical solution (Bear 1972b; Chesnaux 2013), a quadratic regression of the squared saturated soil height against distance was obtained (Fig. 3). The estimated mean groundwater recharge based on a constant parameter—the ratio of recharge to hydraulic conductivity—was 198 mm year^{-1}. This value is comparable to groundwater recharge assessed within other proximal aquifers in the SLSJ region (Boumaiza et al. 2022b); CERM-PACES (2013).

The annual (March 2021–March 2022) fluctuations of water-table elevation within the three piezometers at S1-BER, S2-BER and S4-BER (Fig. 4) were integrated into the WTF-ESPERE automated program to estimate mean annual groundwater recharge. The obtained value was 197 mm year^{-1}, matching the value obtained via the analytical approach. Note that the estimated recharge value of 197 mm year^{-1} (for the period March 2021–March 2022) accounts for 24.2% of the annual (March 2021–March 2022) precipitation registered at a station located approximately 1.5 km northeast of the study site, which indicated a value of 814.5 mm year^{-1} (Government of Quebec 2022). This value of precipitation is 11% less than the historical precipitation average value of 916.3 mm year^{-1} recorded between 2014 and 2021. Consequently, the value of recharge of 197 mm year^{-1} for the period March 2021–March 2022 may slightly underestimate the average historical recharge that would be estimated over the 2014–2021 period. The value of recharge being approximately a quarter of the value of precipitation is expected to be representative of the average regional value of recharge of the aquifer.

Groundwater isotopic signatures

The δ^2H_{H2O} and $\delta^{18}O_{H2O}$ values for the collected groundwater samples ranged from –13.76 to –9.59‰ with a median value of –11.92‰ for $\delta^{18}O$, and from –98.10 to –73.82‰ with a median value of –89.79‰ for δ^2H (Fig. 5). These groundwater isotopic values are comparable to those of Tremblay et al. (2021) who focused on granular aquifers within the Grenville Province and St. Lawrence Platform in southern Québec. The range of stable isotope values for $\delta 2H_{H2O}$ and $\delta 18O_{H2O}$ suggests that the water infiltrated the soil during the warm season. This observation is expected for the study site, as recharge in northern Quebec occurs during the warmer summer–autumn rather than the colder winter–spring when recharge is negligible because of the presence of a snowpack and frozen surface soil acting as a barrier to water infiltration (Boumaiza et al. 2020a, 2021a, b; Boumaiza et al. 2021c; 2022b; Chesnaux and Stumpp 2018).

Table 2 Sediment and groundwater characteristics at the drilled boreholes

Observation well	Ground elevation (m asl)	Stratigraphic unit	Elevation at the base of the unit (m asl)	Water-table elevation (m asl)
S1-BER	179.379	FCBGS-S	171.76	177.63
		CS	171.15	
S2-BER	179.57	FCBGS-S	171.37	177.46
		CS	171.15	
S4-BER	179.88	FCBGS-S	168.30	177.93
		CS	167.69	
PZ-1	182.49	FMGB-S	179.56	180.87
		FCBGS-S	179.19	
PZ-2	180.91	FMGB-S	178.01	179.04
		FCBGS-S	177.10	
PZ-3	180.84	FMGB-S	178.71	179.17
		FCBGS-GS	176.98	
PZ-4	181.34	FMGB-S	177.38	177.96
		FCBGS-GS	176.82	
PZ-5	180.79	FMGB-S	177.79	178.62
		FCBGS-GS	177.22	
PZ-6	181.52	FMGB-S	178.52	179.71
		FCBGS-GS	176.95	
PZ-7	180.19	FMGB-S	176.38	177.61
		FCBGS-GS	175.00	
PZ-9	180.21	FMGB-S	175.33	177.92

asl above mean sea level; *FCBGS-S* fine to coarse brownish-gray sand with traces of silt; *CS* clayey silt; *FMGBS-S* fine to medium gray-brownish sand with traces of silt; *FCBGS-GS* fine to coarse brownish-gray sand with traces of gravel and silt

When the obtained $\delta^{18}O_{H2O}$ and $\delta^{2}H_{H2O}$ are plotted along the PACES-derived local meteoric water line (LMWL), it was noted that they plot around the LMWL, suggesting that the groundwater has been recharged into the BER aquifer through the direct infiltration of precipitation with minimal effect from evaporation (Fig. 5). This pattern is expected for the unconfined aquifer of BER that is dominated by permeable sandy material. The S1-BER and PZ-6 groundwater samples plot slightly below the LMWL, reflecting an effect of evaporation or mixing processes. Evaporation appears to be the dominant process because the calculated groundwater d-excess values (d-excess $= \delta^{2}H_{H2O} - 8\delta^{18}O_{H2O}$) for S1-BER (–2.93‰) and PZ-6 (3‰) are low compared with those of S2-BER (11.63‰) and S4-BER (13.9‰),

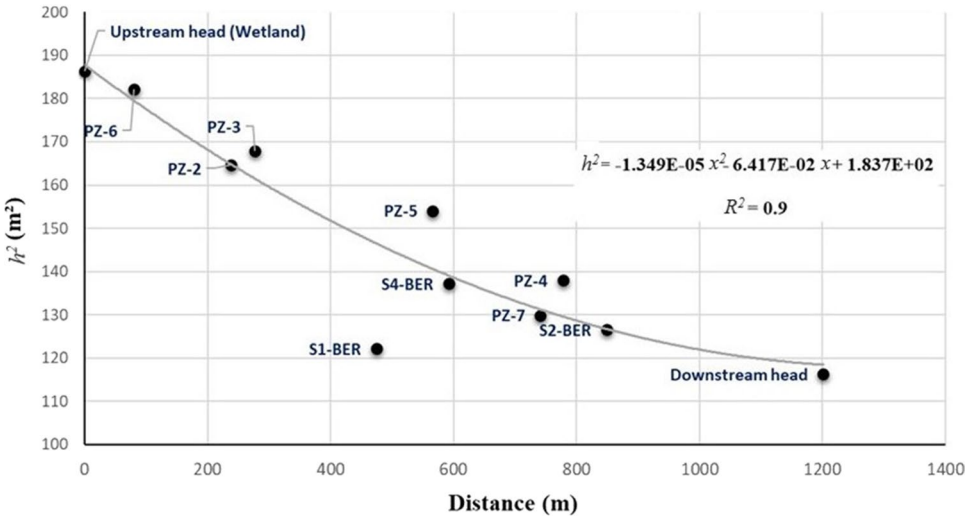

Fig. 3 Quadratic regression of the squared saturated thickness (h^2) along the distance of the cross-section A–A′

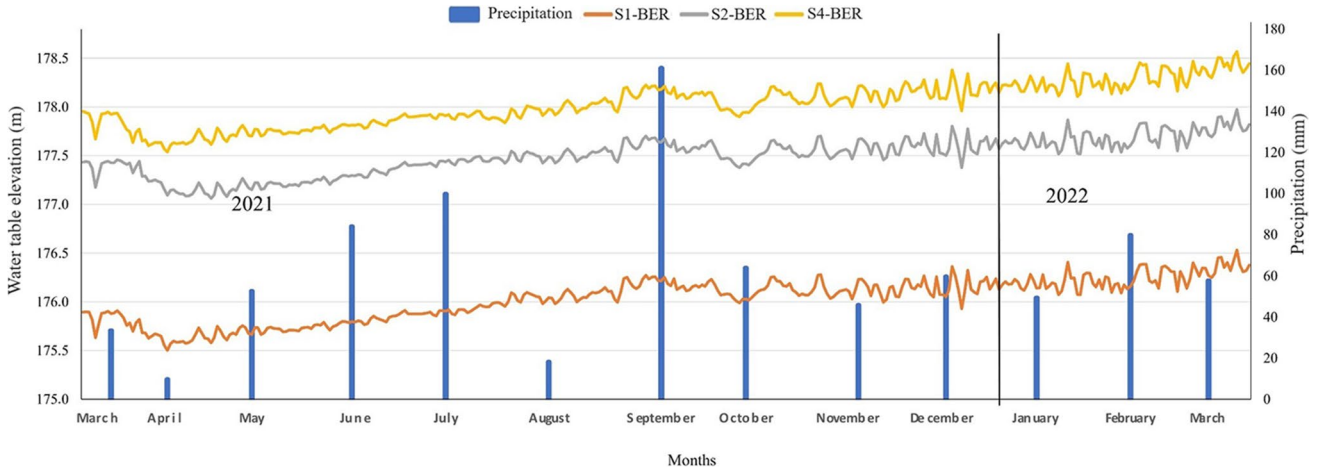

Fig. 4 Elevation of the water levels in boreholes S1-BER, S2-BER, and S4-BER, and precipitation, between March 2021 and March 2022

the latter mostly indicative of a modern recharge that is experiencing a reduced evaporation effect. The water-table elevation variations shown in Fig. 4 confirm the warm summer–autumn recharge, as suggested by δ^2H_{H2O} and $\delta^{18}O_{H2O}$ signatures. The plots illustrate an increased water-table elevation beginning in June because of snow melt and rainfall. Consequently, June was selected for the $a_0{}^3H$ data set when calculating groundwater transit time via the hydrogeochemical approach.

Assessed groundwater transit time

Assessed transit time according to the analytical approach

Because of the homogeneity of the BER aquifer, it is possible to apply the analytical approach to estimate groundwater travel time between the wetland and the discharge zones. The analytical solution of Chesnaux et al. (2005) was used with the upstream head (wetland) and downstream head (discharge point) positioned along a groundwater flow line A–A′ (Fig. 1), involving an east–west groundwater flow across the study site. The eastern boundary condition (wetland) acts as a groundwater divide line, whereas the western imposed boundary represents a groundwater seep (Fig. 2). A groundwater spring was observed at the discharging points during field work. In addition, the studied domain is imposed as homogeneous. Such a flow within the homogeneous sediments of the BER aquifer reflect the Dupuit–Forchheimer flow system conditions, for which groundwater flow is assumed to be under a steady-state regime, unidirectional, and unidimensional within a homogeneous unconfined aquifer constrained by a horizontal substratum. Introducing the

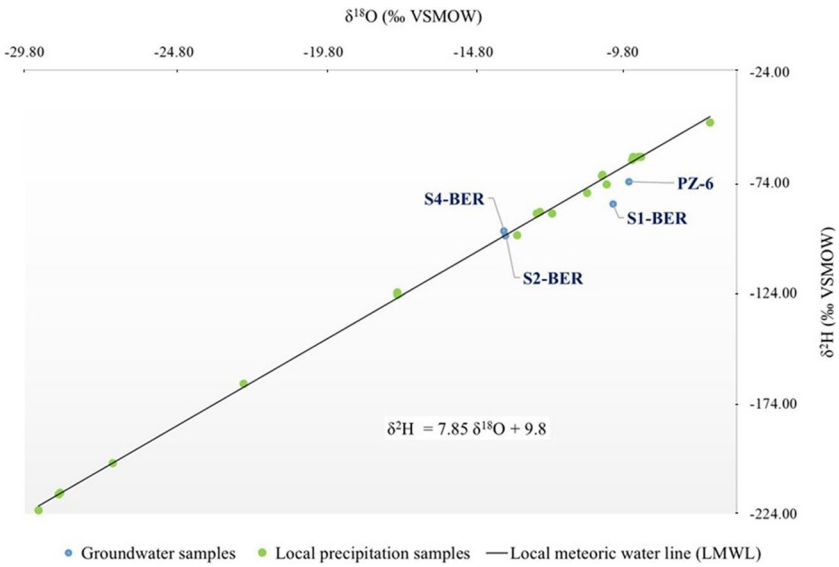

Fig. 5 Distribution of isotopic values of the collected groundwater samples from sites S4-BER, S2-BER, S1-BER, and PZ-6

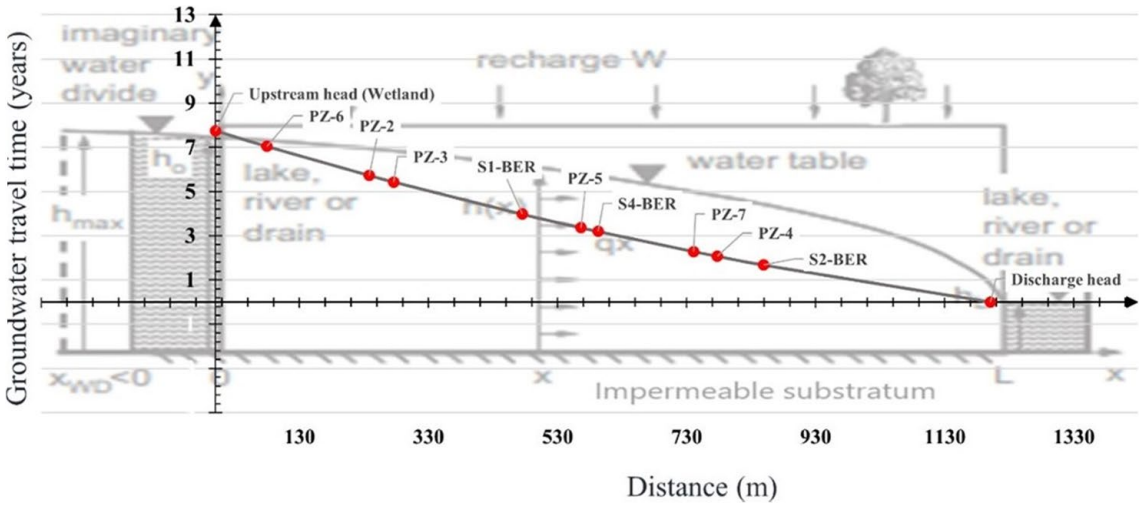

Fig. 6 Illustration of groundwater transit times in the BER aquifer in relation to distance. Background illustration adapted from (Chesnaux et al. 2005)

calculated mean value of the groundwater recharge into the analytical solution along the A–A′ flow line (Fig. 1), the groundwater travel time was calculated from multiple positions (x_i) to the discharge outlet point (Eq. 4). The calculated groundwater travel time from wetland to the discharge point was ~7.75 years, with a relatively consistent time vs. tracking distance along the A–A′ flow line (Fig. 6).

Assessed transit time according to the hydrogeochemical approach

The obtained activities of ^{3}H ($a_t{}^3$H) from the collected groundwater samples are presented in Table 3. The initial ^{3}H activity ($a_0{}^3$H) was set at 9.2 TU, measured from precipitation collected 15 June 2014, a representative month for the potential groundwater recharge period as suggested by δ^2H_{H2O} and $\delta^{18}O_{H2O}$ (i.e., starting from June), and a year (2014) reflecting the transit time yielded by the analytical approach (7.75 years). The transit times were calculated by applying the radioactive decay calculation method (Eq. 8) to the groundwater sample signatures (Table 3). Because there was no sample representing the discharge head directly, S2-BER (located at 351 m from the discharge boundary) was considered as the discharging point. A transit time was calculated from the wetland (recharging point) to the discharging point (S2-BER) of 7.34 years.

Assessed transit time according to the numerical approach

The calibration of the numerical model generated a model mass balance of 1.64×10^{-2}%, and the calculated RMSE was 0.31 m, highlighting the robustness of the fitting process between the simulated and the observed water level data (Fig. 7).

Once calibrated, the model computed the transit time for a particle tracking in the forward direction, i.e., from the wetland to discharge point along the groundwater A–A′ flow line, as presented in Fig. 8. A transit time of 7.27 years was calculated through this approach.

Discussion

Estimates of transit time using the analytical approach involve a number of limitations. These limitations include the uncertainty associated with the input parameters (for

Table 3 Tritium activity and groundwater travel times computed using the hydrogeochemical approach

Sample	$a_t{}^3$H (TU)	Date of $a_t{}^3$H sample	$a_0{}^3$H (TU)	Date of $a_0{}^3$H sample	Transit time (years)
PZ-6	9	2021–12-10	9.2	2014–06-15	0.31
S2-BER	6.1	2021–12-14	9.2	2014–06-15	7.34
S4-BER	6.5	2021–12-14	9.2	2014–06-15	6.09

Tritium is reported in tritium units (TU); 1 TU = 3.221 pCi L^{-1}

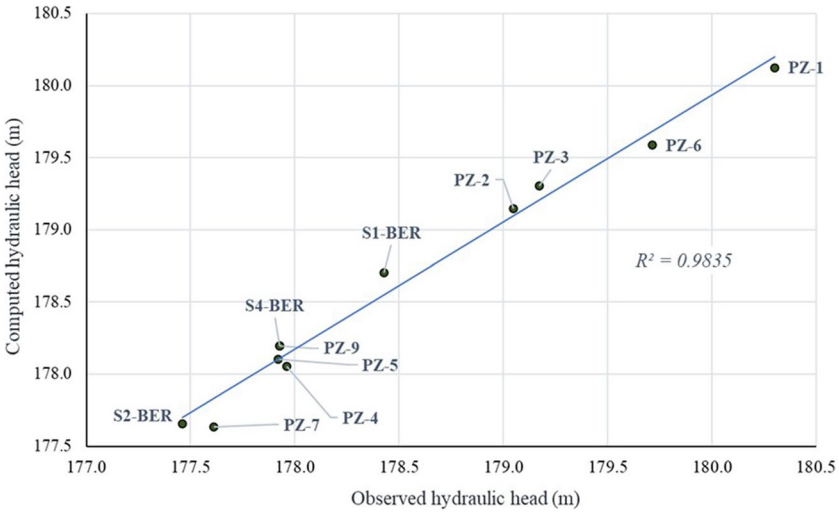

Fig. 7 Relationship between the observed and computed hydraulic heads (m above sea level)

use of Eq. 4), including hydraulic conductivity, groundwater recharge, and porosity. Furthermore, the restrictive assumptions associated with a Dupuit–Forchheimer flow type aquifer produce simplistic albeit realistic features of the study site. For instance, contaminant transport is affected by multiple natural processes (Bradley 2013; Gorelick et al. 1993) and can be subjected to diverse transportation processes, e.g., diffusion and dispersion, rather than only advection as assumed in this study. Moreover, infiltration through the vadose zone can influence groundwater transit time (Boumaiza et al. 2021a), whereas the analytical and numerical approaches used here limit groundwater flow to only the saturated zone. Thus, the assessed groundwater transit time is less certain when using the analytical and numerical approaches reported here. Sousa et al. (2013) and Wang et al. (2012) demonstrated that aquifers having a thick vadose zone exhibit a much longer groundwater transit time in this zone; for example (Schwientek et al. 2009; Zoellmann et al. 2001) found that unsaturated zones greater than 10 m thick affected groundwater transit times. Given that the BER site has a thin unsaturated zone (0.5–2 m), it is believed that any vadose zone effects on transit time are negligeable.

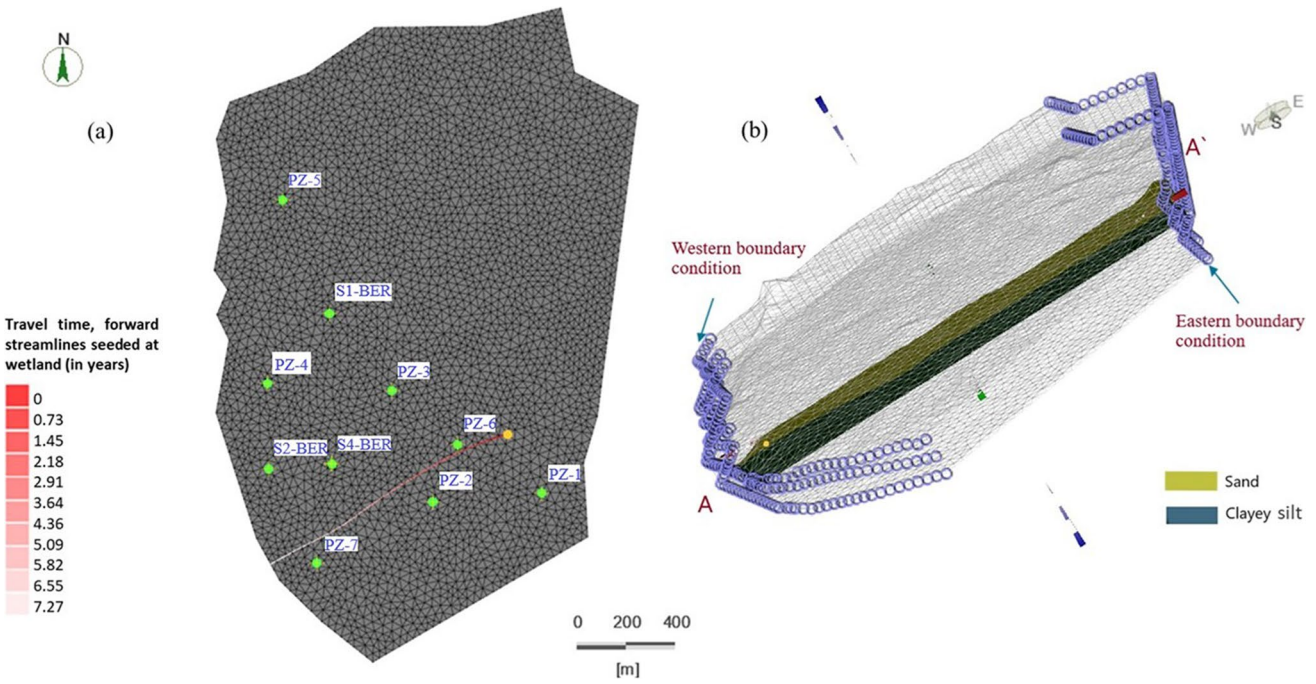

Fig. 8 **a** A one-dimensional (1D) representation of the domain modeled by using the FEFLOW model. The traced line is the tracking path, and the transit time in years is indicated in the legend; **b** a 3D perspective of the studied aquifer

The hydrogeochemical approach determined that the groundwater transit time was 7.34 years, slightly less than that obtained via the analytical method (7.75 years). This subtle difference may stem from S2-BER being considered as the discharge point. This point is 350 m distant from the actual downstream head boundary, as considered in the analytical model. Moreover, ^{3}H activity and the associated transit times (Table 3) agree with published values. Indeed, Clark and Fritz (1997) indicate that for continental regions, as is the case of the study site, ^{3}H concentrations between 5 and 15 TU correspond to modern recharge (<5–10 years).

Nonetheless, the hydrogeochemical approach relies on a simple model, which is not a typical characteristic of natural systems. This approach assumes that three samples are sufficient for obtaining an accurate transit time, and this approach does not consider possible mixing processes during the recharge and infiltration (Michel 2005). As shown by Małoszewski et al. (1983) and Vitvar and Balderer (1997), the use of isotopes and solutes is limited by short data time series, which provides little insight into the temporal variation of transit times. Moreover, because the ^{3}H concentrations of remnant bomb pulse waters in the Northern Hemisphere are currently greater than concentrations in modern rainfall, it is increasingly necessary to estimate transit times using ^{3}H-level time series (Morgenstern et al. 2010). (Clark and Fritz 1997) recommend to ideally use a ^{3}H input representing a multiyear average and applying an input function calculated via a model that incorporates mixing and decay into the recharge process.

The numerical approach yielded a transit time of 7.27 years, slightly shorter than that of the analytical and hydrogeochemical approaches. A source of error in the numerical approach involves uncertainties and insufficiencies in the input data. Although these inputed parameters are the same as those of the analytical approach, it appears that the calibrating process involving a change in these input parameters affects the estimated transit time.

Furthermore, advection is also assumed to be the main transport mechanism for the particle-tracking computation. Therefore, in cases where dispersion is expected to play an important role, this approach may not be very applicable; however, in terms of contaminant transport, this method is suited for conservative solutes because other biogeochemical reactions are not explicitly considered.

Moreover, actual aquifer depths recorded during field observations were used in the FEFLOW 3D model; therefore, the 3D model does not present a perfectly horizontal substratum as assumed by the Dupuit–Forchheimer system. This difference could explain the variation between the two results. In the analytical model, it was assumed that the saturated thickness of the aquifer was uniform, an assumption does not necessarily reflect the actual geological conditions. Indeed, the base of the aquifer forms a slight slope (Figs. 1 and 8b), leading to a variable saturated zone thickness. Because the thickness of the saturated aquifer affects both the transit path track and the horizontal hydraulic gradients (Haitjema 1995), the longer transit time estimated by the analytical approach, relative to that of the numerical approach, can be attributed to uncertainties in the initial estimates of saturated aquifer thickness. This discrepancy demonstrates the challenge in considering a representative saturated thickness for an unconfined aquifer, especially at larger scales. Therefore, the analytical solution proposed by Chesnaux et al. (2005) appears valid under conditions of an idealized unconfined aquifer with a slight variation in head relative to the saturated aquifer thickness.

All three methods required significant amounts of field data. The analytical approach was the least complex and the least time-consuming once these data were available, whereas the numerical approach required the most time investment to learn the software and involved laborious computational resources. Finally, the geochemical approach was of intermediate complexity because of the waiting period for the results, although their interpretation was not time consuming. Consequently, if the main goal is the approximate and prompt estimation of transit time, the analytical solution provides the best approach.

Conclusion

Analytical, hydrogeochemical, and numerical approaches were combined in a multi-technique framework to estimate advective groundwater transit time in a granular unconfined aquifer. Transit time represented the time for groundwater to be transported from a wetland to the discharge zone of the aquifer. Realistic soil physical properties were integrated into the analytical and numerical approaches and used ^{3}H-groundwater isotopes in the hydrogeochemical approach. Estimated groundwater transit times varied from 7.27 to 7.75 years for the three approaches, demonstrating the advantage of combining several approaches using field data to estimate groundwater transit time. Further studies are required to estimate groundwater transit time through the vadose zone; these results would allow tracking groundwater movement from the ground surface to the discharge point.

This study aimed to estimate the transit time of potential contamination generated from an agricultural field to the nearby river, using groundwater transit time as an analog of contaminant transit time and assuming a simple transport advective mechanism. Additional studies should consider other processes affecting contaminant transport, such as dispersion, diffusion, sorption, and degradation. Nonetheless, the study provides a valuable contribution to understanding the behaviour of the BER aquifer and to improving the

management of groundwater resources of this aquifer. Also, it can be underlined that the methodology applied in this study could be applied to larger aquifers where high-resolution field data cannot be collected. In this case, it is suggested to use remote sensing data such as satellite imagery, or geophysical data that can provide information on larger areas in aquifers. These data can be used to calibrate models and validate the results (Lévesque et al. 2023). Finally, while high-resolution field data may not be obtained for the entire aquifer, it may be possible to collect data at a few strategic locations that can be representative of a larger extent of the aquifer.

Supplementary information The online version contains supplementary material available at https://doi.org/10.1007/s10040-023-02663-0.

Acknowledgements The authors thank David Noël for his greatly appreciated help and guidance during field work and Mike Bellemare, Laura-Pier Perron Desmeules, and Pier-Olivier Gilbert for their assistance during field work.

Funding The authors thank Mitacs Globalink Graduate Fellowship Program,Canada (IT17061), Fonds d'appui au rayonnement des régions (FARR), and Fondation de l'Université du Québec à Chicoutimi (FUQAC) for financial support.

Declarations

Conflict of interests The authors declare that they have no known competing financial interests or personal relationships that could have appeared to influence the work reported in this paper.

References

Aggarwal PK, Araguás-Araguás LJ, Groening M, Kulkarni KM, Kurttas T, Newman BD, Vitvar T (2010) Global hydrological isotope data and data networks. In: Isoscapes. pp 33–50. https://doi.org/10.1007/978-90-481-3354-3_2

Anderson MP, Woessner WW, Hunt RJ (2015) Particle tracking. chap 8. In: Applied groundwater modeling: simulation of flow and advective transport. Academic, San Diego, CA

Basu NB, Jindal P, Schilling KE, Wolter CF, Takle ES (2012) Evaluation of analytical and numerical approaches for the estimation of groundwater travel time distribution. J Hydrol 475:65–73

Bear J (1972a) Dynamics of fluids in porous media, part 1. Elsevier, New York

Bear J (1972b) Dynamics of fluids in porous media, part 2. Elsevier, New York

Bear J (1988) Dynamics of fluids in porous media. Courier, Chelmsford, MA

Bethke CM, Johnson TM (2008) Groundwater age and groundwater age dating. Annu Rev Earth Planet Sci 36:121–152

Beyer W (1964) Zur Beschreibung der Wasserdurchlässigkeit von Kiesen und Sanden [To describe the water permeability of gravel and sand]. Zeitschr Wasserwirtsch-Wassertechn 14:165–168

Black CA (ed) (1965) Methods of soil analysis, part 1: physical and mineralogical properties, including statistics of measurement and sampling. American Society of Agronomy, Madison, WI

Boumaiza L (2008) Caractérisation hydrogéologique des hydrofaciès dans le paléodelta de la rivière Valin au Saguenay [Hydrogeological characterization of hydrofacies in the Valin River paleodelta at Saguenay]. Université du Québec à Chicoutimi, Chicoutimi, QC

Boumaiza L, Rouleau A, Cousineau P (2015) Estimation de la conductivité hydraulique et de la porosité des lithofaciès identifiés dans les dépôts granulaires du paléodelta de la rivière Valin dans la région du Saguenay au Québec [Estimation of hydraulic conductivity and porosity of lithofacies identified in Valin River paleodelta granular deposits in the Saguenay region of Quebec]. In: Proceedings of the 68th Canadian Geotechnical Conference, vol 9, Quebec City, Quebec, Canada, September 2015

Boumaiza L, Rouleau A, Cousineau P (2017) Determining hydrofacies in granular deposits of the Valin River paleodelta in the Saguenay region of Quebec. In: Proceedings of the 70th Canadian Geotechnical Conference and the 12th Joint CGS/IAH-CNC Groundwater Conference, vol 8, Ottawa, ON, October 2017

Boumaiza L, Rouleau A, Cousineau P (2019) Combining shallow hydrogeological characterization with borehole data for determining hydrofacies in the Valin River paleodelta. In: Proceedings of the 72nd Canadian Geotechnical Conference, vol 8, St-John's, NL

Boumaiza L, Chesnaux R, Walter J, Stumpp C (2020a) Assessing groundwater recharge and transpiration in a humid northern region dominated by snowmelt using vadose-zone depth profiles. Hydrogeol J 28:2315-2329

Boumaiza L, Chesnaux R, Walter J, Stumpp C (2020b) Assessing groundwater recharge and transpiration in a humid northern region dominated by snowmelt using vadose-zone depth profiles. Hydrogeol J 28:2315-2329. https://doi.org/10.1007/s10040-020-02204-z

Boumaiza L, Chesnaux R, Drias T, Walter J, Huneau F, Garel E, Knoeller K, Stumpp C (2020c) Identifying groundwater degradation sources in a Mediterranean coastal area experiencing significant multi-origin stresses. Sci Total Environ 746:141203

Boumaiza L, Chesnaux R, Walter J, Stumpp C (2021a) Constraining a flow model with field measurements to assess water transit time through a vadose zone. Groundwater 59:417–427

Boumaiza L, Chesnaux R, Walter J, Meghnefi F (2021b) Assessing response times of an alluvial aquifer experiencing seasonally variable meteorological inputs. Groundw Sustain Dev 14:100647

Boumaiza L, Walter J, Chesnaux R, Brindha K, Elango L, Rouleau A, Wachniew P, Stumpp C (2021c) An operational methodology for determining relevant DRASTIC factors and their relative weights in the assessment of aquifer vulnerability to contamination. Environ Earth Sci 80:1–19

Boumaiza L, Chesnaux R, Walter J, Lenhard RJ, Hassanizadeh SM, Dokou Z, Alazaiza MY (2022a) Predicting vertical LNAPL distribution in the subsurface under the fluctuating water table effect. Groundwater Monit Remediat 42:47–58

Boumaiza L, Walter J, Chesnaux R, Lambert M, Jha MK, Wanke H, Brookfield A, Batelaan O, Galvão P, Laftouhi NE (2022b) Groundwater recharge over the past 100 years: regional spatiotemporal assessment and climate change impact over the Saguenay-Lac-Saint-Jean region Canada. Hydrol Processes 36:e14526

Bradley P (2013) Current perspectives in contaminant hydrology and water resources sustainability. InTech, Rijeka, Croatia

Cartwright I, Morgenstern U (2015) Transit times from rainfall to baseflow in headwater catchments estimated using tritium: the Ovens River, Australia. Hydrol Earth Syst Sci 19:3771–3785

Cartwright I, Morgenstern U (2016) Using tritium to document the mean transit time and sources of water contributing to a chain-of-ponds river system: implications for resource protection. Appl Geochem 75:9–19

CERM-PACES (2013) Résultats du programme d'acquisition de connaissances sur les eaux souterraines du Saguenay-Lac-Saint-Jean. Université du Québec à Chicoutimi, Chicoutimi, QC

Chapuis RP (2004) Predicting the saturated hydraulic conductivity of sand and gravel using effective diameter and void ratio. Can Geotech J 41:787–795

Chesnaux R (2013) Regional recharge assessment in the crystalline bedrock aquifer of the Kenogami Uplands, Canada. Hydrol Sci J 58:421–436

Chesnaux R, Stumpp C (2018) Advantages and challenges of using soil water isotopes to assess groundwater recharge dominated by snowmelt at a field study located in Canada. Hydrol Sci J 63:679–695

Chesnaux R, Molson J, Chapuis R (2005) An analytical solution for ground water transit time through unconfined aquifers. Groundwater 43:511–517

Chesnaux R, Marion D, Boumaiza L, Richard S, Walter J (2021) An analytical methodology to estimate the changes in fresh groundwater resources with sea-level rise and coastal erosion in strip-island unconfined aquifers: illustration with Savary Island, Canada. Hydrogeol J 29:1355–1364

Clark ID, Fritz P (1997) Environmental isotopes in hydrogeology. Routledge, Abingdon, UK, 328 pp

Cook PG, Böhlke J-K (2000) Determining timescales for groundwater flow and solute transport. In: Environmental tracers in subsurface hydrology. Springer, Heidelberg, Germany, pp 1–30

Cook PG, Herczeg AL (2012) Environmental tracers in subsurface hydrology. Springer, Heidelberg, Germany

Cornaton F (2003) Deterministic models of groundwater age, life expectancy and transit time distributions in advective-dispersive systems. Université de Neuchâtel, Neuchâtel, Switzerland

Courchesne C (2019) Caractérisation hydrogéologique de la bleuetière d'enseignement et de recherche Secteur Normandin, Québec [Hydrogeological characterization of the teaching and research blueberry farm Secteur Normandin, Québec]. Université du Québec à Chicoutimi, Chicoutimi, QC

Diersch H-JG (2013) FEFLOW: finite element modeling of flow, mass and heat transport in porous and fractured media. Springer, Heidelberg, Germany

Dupuit JE (1863) Etudes théoriques et pratiques sur le mouvement des eaux dans les canaux découverts et à travers les terrains perméables avec des considérations relatives au régime des grandes eaux, au débouché à leur donner, et à la marche des des alluvions dans les rivières à fond mobile [Theoretical and practical studies on the movement of water in open canals and through permeable terrain with considerations relating to the regime of large waters, the outlet to be given to them, and the movement of alluvial deposits in rivers with mobile bottoms]. Dunod, Paris

Ekwurzel B, Schlosser P, Smethie WM Jr, Plummer LN, Busenberg E, Michel RL, Weppernig R, Stute M (1994) Dating of shallow groundwater: comparison of the transient tracers 3H/3He, chlorofluorocarbons, and 85Kr. Water Resour Res 30:1693–1708

Etcheverry D, Perrochet P (2000) Direct simulation of groundwater transit-time distributions using the reservoir theory. Hydrogeol J 8:200–208

Fontes J-C (1992) Chemical and isotopic constraints on 14 C dating of groundwater. In: Radiocarbon after four decades. Springer, Heidelberg, Germany, pp 242–261

Forchheimer P (1886) Uber die Ergiebigkeit von Brunnenanlagen and Sickershlitzen [About the yield of wells and seepage systems]. Z. Arch. Ing. Verein, Hannover, 32

Gardner WH (1965) Water content. In: Methods of soil analysis: part 1, physical and mineralogical properties, including statistics of measurement and sampling. Agronomy Monographs Series 9, Wiley, Chichester, UK, pp 82–127

Gillon M, Barbecot F, Gibert E, Plain C, Corcho-Alvarado J-A, Massault M (2012) Controls on ^{13}C and ^{14}C variability in soil CO2. Geoderma 189:431–441

Goode DJ (1996) Direct simulation of groundwater age. Water Resour Res 32:289–296

Gorelick SM, Freeze RA, Donohue D, Keely JF (1993) Groundwater contamination: optimal capture and containment. Lewis, New York

Government of Quebec (2022) Normales climatiques du Québec 1981–2010. https://www.environnement.gouv.qc.ca/climat/normales/climat-qc.htm. Accessed October 2021

Haitjema HM (1995) Analytic element modeling of groundwater flow. Elsevier, Amsterdam

Hazen A (1983) Some physical properties of sand and gravel with special reference to their use in filtration. 24th Ann. Rep., Mass. State Board of Health, Boston

Healy RW, Cook PG (2002) Using groundwater levels to estimate recharge. Hydrogeol J 10:91–109

Hudon-Gagnon E, Chesnaux R, Cousineau PA, Rouleau A (2011) A methodology to adequately simplify aquifer models of quaternary deposits: preliminary results. GeoHydro 2011

Labrecque Gv, Chesnaux R, Boucher M-Al (2020) Water-table fluctuation method for assessing aquifer recharge: application to Canadian aquifers and comparison with other methods. Hydrogeol J 28:521–533

Lanini S, Caballero Y (2021) ESPERE, a tool for multimethod aquifer recharge estimation: what's new with version 2? Groundwater 59:5–6

Lanini S, Caballero Y, Seguin J-J, Maréchal J-C (2016) ESPERE: a multiple-method Microsoft Excel application for estimating aquifer recharge. Groundwater 54:155–156

Larocque M, Levison J, Martin A, Chaumont D (2019) A review of simulated climate change impacts on groundwater resources in Eastern Canada. Can Water Resour J/Rev Can Ressour Hydri 44:22–41

LaSalle P, Tremblay G (1978) Dépôts meubles Saguenay-Lac-Saint-Jean [Saguenay-Lac-Saint-Jean granular deposits]. Report 19, Ministry of Natural Resources, Quebec, QC

Lefebvre K, Barbecot F, Larocque M, Gillon M (2015) Combining isotopic tracers (222Rn and δ13C) for improved modelling of groundwater discharge to small rivers. Hydrol Process 29:2814–2822

Leray S, De Dreuzy J-R, Bour O, Labasque T, Aquilina L (2012) Contribution of age data to the characterization of complex aquifers. J Hydrol 464:54–68

Lévesque Y, Chesnaux R, Walter J (2023) Using geophysical data to assess groundwater levels and the accuracy of a regional numerical flow model. Hydrogeol J 31:351–370

Małoszewski P, Rauert W, Stichler W, Herrmann A (1983) Application of flow models in an alpine catchment area using tritium and deuterium data. J Hydrol 66:319–330

Mazariegos JG, Walker JC, Xu X, Czimczik CI (2017) Tracing artificially recharged groundwater using water and carbon isotopes. Radiocarbon 59:407–421

Mazor E (2003) Chemical and isotopic groundwater hydrology. CRC, Boca Raton, FL

McCarthy J, Zachara J (1989) ES&T Features: Subsurface transport of contaminants. Environ Sci Technol 23:496–502

McGuire KJ, McDonnell JJ (2006) A review and evaluation of catchment transit time modeling. J Hydrol 330:543–563

Michel RL (2005) Tritium in the hydrologic cycle. In: Isotopes in the water cycle. Springer, Heidelberg, Germany, pp 53–66

Milan V, Andjelko S (1992) Determination of hydraulic conductivity of porous media from grain-size composition. No. 551.49 V 986, Water Resources, Littleton, CO

Morgenstern U, Stewart MK, Stenger R (2010) Dating of streamwater using tritium in a post nuclear bomb pulse world: continuous variation of mean transit time with streamflow. Hydrol Earth Syst Sci 14:2289–2301

Navfac D (1974) Design manual: soil mechanics, foundations, and earth structures. US Government Printing Office, Washington, DC

Nastev M, Rivera A, Lefebvre R, Martel R, Savard M (2005) Numerical simulation of groundwater flow in regional rock aquifers, southwestern Quebec, Canada. Hydrogeol J 13:835–848

Nimmo JR, Horowitz C, Mitchell L (2015) Discrete-storm water-table fluctuation method to estimate episodic recharge. Groundwater 53:282–292

Penna D, Stenni B, Šanda M, Wrede S, Bogaard T, Gobbi A, Borga M, Fischer B, Bonazza M, Chárová Z (2010) On the reproducibility and repeatability of laser absorption spectroscopy measurements for δ^2H and $\delta^{18}O$ isotopic analysis. Hydrol Earth Syst Sci 14:1551–1566

Ritter KS, Sibley P, Hall K, Keen P, Mattu G, Linton B, Len. (2002) Sources, pathways, and relative risks of contaminants in surface water and groundwater: a perspective prepared for the Walkerton inquiry. J Toxicol Environ Health A 65:1–142

Sauerbrey I (1932) On the problem and determination of the permeability coefficient. Proceedings B.E. Vedeneev All-Russia Research Institute Of Hydraulic Engineering (VNIIG), pp 115–145

Schwientek M, Maloszewski P, Einsiedl F (2009) Effect of the unsaturated zone thickness on the distribution of water mean transit times in a porous aquifer. J Hydrol 373:516–526

Seequent (2022) Leapfrog Geo 2021.2.5 help and support. https://www.seequent.com/help-support/leapfrog-geo/. Accessed January 2022

Sousa MR, Jones JP, Frind EO, Rudolph DL (2013) A simple method to assess unsaturated zone time lag in the travel time from ground surface to receptor. J Contam Hydrol 144:138–151

Taylor C (1976) Tritium enrichment of environmental waters by electrolysis: development of cathodes exhibiting high isotopic separation and precise measurement of tritium enrichment factors. Technical report no. INIS-XA-73, IAEA, Vienna

Tremblay R, Walter J, Chesnaux R, Boumaiza L (2021) Investigating the potential role of geological context on groundwater quality: a case study of the Grenville and St. Lawrence platform geological provinces in Quebec, Canada. Geosciences 11:503

Vitvar T, Balderer W (1997) Estimation of mean water residence times and runoff generation by 180 measurements in a Pre-Alpine catchment (Rietholzbach, eastern Switzerland). Appl Geochem 12:787–796

Vogel J (1967) Investigation of groundwater flow with radiocarbon: In: Isotopes in Hydrology. International Atomic Energy Agency, Vienna

Wang L, Stuart M, Bloomfield J, Butcher A, Gooddy D, McKenzie A, Lewis M, Williams A (2012) Prediction of the arrival of peak nitrate concentrations at the water table at the regional scale in Great Britain. Hydrol Process 26:226–239

Wentworth CK (1922) A scale of grade and class terms for clastic sediments. J Geol 30:377–392

Zappa G, Bersezio R, Felletti F, Giudici M (2006) Modeling heterogeneity of gravel-sand, braided stream, alluvial aquifers at the facies scale. J Hydrol 325:134–153

Zedler JB, Kercher S (2005) Wetland resources: status, trends, ecosystem services, and restorability. Annu Rev Environ Resour 30:39–74

Zoellmann K, Kinzelbach W, Fulda C (2001) Environmental tracer transport (3H and SF6) in the saturated and unsaturated zones and its use in nitrate pollution management. J Hydrol 240:187–205